Assessment of Energy-Saving Potential of an Automated Ion-Exchange System in Hydrogen Conductivity Measurement at Thermal Power Plants

Tianbo Ma[1], Le Chen[1*], Heng Jiang[1], Yachao Li[1], Xuebin Yang[1], Honglei Cui[1], Jun Zhang[1]
[1]Department of State Gnid-Energy Hami Coal & Power Co.,Ltd Huayuan Power Plant, Hami 839000, Xinjiang, China
Corresponding author: Le Chen (e-mail: 13955416142@163.com).

ABSTRACT To overcome the problems of acid regeneration of the conventional cation exchange resin (CXR) column, long flushing time, high labor hours for maintenance and high consumption of resources involved in hydrogen conductivity measurement in a thermal power plant, an automated ion exchange system was designed and validated at 20 water and steam measurement points of Units 1 and 3 of a coal-fired power plant. It combines the continuous electrical regeneration with closed loop flow control, on line parameter acquisition and fault protection logic. An energy-saving potential evaluation model was created for resin, hydrochloric acid, rinse water, waste liquid, labour hours and operational electricity consumption. The results indicate that the NH_4^+ removal rate remained stable at 99.90%–99.94%, the stabilization time of the hydrogen conductivity was shortened from 44-76 min to 12-19 min and the annualized operation and maintenance cost decreased from from 166, 800 CNY/year to 23, 600 CNY/year (reduction rate 85.9%). Automated continuous electro-regeneration ion exchange (CEIX) is a reliable, quantifiable and low energy consumption pretreatment system for continuous hydrogen conductivity measurement in thermal power plants.

INDEX TERMS Automated ion exchange; hydrogen conductivity measurement; continuous electrogeneration; thermal power plant; water and steam chemistry monitoring

I. INTRODUCTION

Hydrogen conductivity is one of the most important parameters for identifying anion pollution and evaluating the risk of corrosion and scale formation in the chemical monitoring of thermal power stations. Nowadays, the international research has changed from single parameter conductivity monitoring to multi-parameter collaborative identification. Nakatsuchi et al. established a method for identifying seawater leakage based on pH, specific conductivity, and cation conductivity, demonstrating that conductivity-based indicators still hold irreplaceable value for online monitoring in diagnosing contamination in water and steam circuits [1].At the same time, the stability of corrosion inhibitors in high-temperature water and steam environments, as well as the impact of alternative reducing agents on water quality and carbon steel corrosion, continue to attract attention. Relevant studies emphasize that water chemistry control must balance measurement accuracy, corrosion control, and long-term operational stability [2–3].Against this backdrop, the reliability of the pretreatment stage in hydrogen conductivity measurements directly affects the results of anion impurity analysis. Traditional cation exchange resins are prone to measurement lags or short-term deviations due to fluctuations in regeneration efficiency, prolonged rinsing times, and variations in manual maintenance.

In recent years, the rapid development of electrodialysis, bipolar membrane electrodialysis, and cation exchange membrane technologies has provided a new technical foundation for ion migration, selective separation, and online regeneration. Cassaro et al. validated the feasibility of acid and alkali production via bipolar membrane electrodialysis at the pilot scale, while Herrero-Gonzalez et al. further analyzed the impact of operating parameters on acid and alkali yields, demonstrating that electrically driven membrane processes have progressed from laboratory research to the stage of engineering optimization [4–5].Virruso et al. evaluated the operational performance of a pilot-scale bipolar membrane electrodialysis unit based on feed and product circulation modes; Tekinalp et al. systematically summarized process optimization issues for cation exchange membranes in selective metal separation; and Kikuchi et al. analyzed conditions for efficient operation for different ion types and membrane combinations [6–8].Collectively, these studies show that the ion migration, selective membrane

transport, and the control of operational parameters are the basis of continuous ion exchange and regeneration. Meanwhile, studies on the application of electrodialysis in chemical processes and brackish water desalination have demonstrated that there is measurable scope for optimization in terms of energy consumption, operational stability, and engineering costs. [9–10]. Current research focuses mainly on membrane separation mechanisms, acid and alkali generation, desalination, and corrosion control; however, there is still a lack of field validation for automatic ion exchange, continuous electrogeneration and energy saving potential assessment, which is aimed at pretreating hydrogen conductivity measurements in thermal power plants. The system integrates continuous electric regeneration, closed loop flow control, on-line parameter collection, and fault protection logic into the pre-process of hydrogen conductivity measurement. In addition, a comprehensive energy saving assessment method has been developed, covering resin, hydrochloric acid, wash water, waste fluid, working time, and operating power consumption. It has developed a technology roadmap spanning from ion exchange mechanism to engineering and economy calculations, which will provide the basis for low energy and smart updating of the instrument.

II. MATERIALS AND METHODS

A. FIELD APPLICATION TARGETS AND MEASUREMENT POINT CONFIGURATION

The field application focused on the water and steam sampling system and the Polishing treatment area of units 1 and 3 at Huayuan Power Plant, covering 20 measuring points of hydrogen conductivity, including condensate, feedwater, vapor, and fine processing outlets.The original hydrogen conductivity measuring unit was kept at each measuring point; only the pretreating unit upstream of the cation exchange resin column was replaced by an automatic ion exchange unit, forming a sequence process of "raw water-electroregenerated ion exchange — Hydrogen conductivity measurement — data recording." A 5-inch filter is installed at the inlet of the sample, with an inlet pressure of 0.20 to 0.25 MPa; when the pressure exceeds this limit, the system is switched to a pressure-stabilizing protective arm [11]. The monitoring points are separated into feed, vapour and fine processing areas, depending on the water/steam flow procedure, which corresponds to a high level of ammonia disturbance, the detection of anion anomalies and the verification of the quality of the effluent effluent, etc. The data is sent to the edge data collection module through the RTU-485. For normal operation parameters, a sampling interval of 60 seconds is set, and a sampling interval of 1 – 5 s for protection parameters, for example pressure, water supply interruption, and overpressure, is set to 1 – 5 s to evaluate continuous operating stability and to calculate energy savings. Specific parameters are shown in Table 1.

B. COMPOSITION OF THE AUTOMATED ION EXCHANGE SYSTEM

As shown in Figure 1, the automatic ion exchange system consists of four functions: the pretreating of the sample water, the continuous Electro-regenerated ion exchange, the closed loop flow control, the state monitoring and the data communication. At the inlet of the sample, a particulate filter unit and a pressure-distributing branch are installed. Channel A serves as a regeneration feed and a hydrogen conductivity measuring channel; Channel E is a waste water channel; port D is used to discharge waste water; port C is used for overpressure protection. The pipeline is designed for a low flow rate and minimum dead volume to minimize the influence of the replacement time on hydrogen conductivity. The core processing unit is composed of an electroregenerative ion module, a direct current source module, a flow transducer, a control valve, a pressure detecting section, a 4.3 inch touch screen, and a communication interface of RTU-485. The electroregeneration module uses direct current electrolysis to produce H^+ and OH^-; H^+ is transferred to the resin side via the exchange membrane, continuously regenerating the exhausted resin, and at the same time, displacing cations such as NH_4^+, Na^+, Ca^{2+}, Mg^{2+}, and Na+ from the sample water.The controller performs variable frequency regeneration and detection based on the feed water pressure, the regeneration rate, the wastewater flow rate, the voltage, the current, and the PIV state. The system is powered by AC 220 V $\pm$ 22 V, with a designed regeneration voltage of DC 5 – 24 V, a total feed water flow rate of 100 – 300 mL/min, an RTU-485 communication interface, and an IP65 protection rating [12].

C. CONTINUOUS ELECTRO-REGENERATION AND CLOSED-LOOP FLOW CONTROL METHOD

The continuous electric regeneration unit drives the electrolysis of water and the migration of ions by direct current. During the operation, the resin columns are not removed, and no hydrochloric acid is added. The H ions produced by the electrolysis flow into the resin side and displace the cations such as NH, Na, Ca, Na, Ca, Na, Ca, and Na from the resin exchange site. Under the effect of the electric field and the concentration gradient, the displaced cations are transferred to the waste water side and are discharged from the port D. The ion migration potential across the membrane is verified using the following equation:

$$\Delta V = \frac{RT}{zF} \ln\left(\frac{a_1}{a_2}\right) \tag{1}$$

In the equation, ΔV represents the potential difference required for ion migration across the membrane; R is the gas constant; T is the absolute temperature; z is the valence of the migrating ion; F is the Faraday constant; and a_1 and a_2 are the ionic activities on either side of the membrane, respectively. This equation is used to determine if the setting of the regeneration voltage meets the conditions for the

TABLE 1. Table of field measurement points and operating conditions for hydrogen conductivity measurement in thermal power plants

Point Category	Typical Measurement Points	System	Sample Water Pressure/MPa	Sample Water Temperature/°C	Design Sample Water Flow Rate/(mL·min^{-1})	Specific Conductivity Control Range/(μS·cm^{-1})	Data Acquisition Interval
Condensate Side	Hydrogen Conductivity at Condensate Pump Outlet	Steam-water sampling system	$\geq$0.20; protection triggered at $>$ 0.25	10–35	$>$ 100	$<$ 15	60 s
Feedwater side	Hydrogen conductivity at deaerator inlet	Steam-water sampling system	$\geq$0.20; protection triggered if $>$ 0.25	10–35	$>$ 100	$<$ 15	60 s
Feedwater side	Hydrogen conductivity at economizer inlet	Steam-water sampling system	$\geq$0.20; protection triggered if $>$ 0.25	10–35	$>$ 100	$<$ 15	60 s
Steam side	Main Steam Hydrogen Conductivity	Steam-water sampling system	$\geq$0.20; protection if $>$ 0.25	10–35	$>$ 100	$<$ 15	60 s
Steam side	Reheated Steam Hydrogen Conductivity	Steam-water sampling system	$\geq$0.20, protection if $>$ 0.25	10–35	$>$ 100	$<$ 15	60 s
Drain side	Start-up separator drain hydrogen conductivity	Steam-water sampling system	$\geq$0.20; protection triggered if $>$ 0.25	10–35	$>$ 100	$<$ 15	60 s
Refined treatment side	Total hydrogen conductivity at the fine treatment outlet	Fine Treatment System	$\geq$0.20; protection triggered if $>$ 0.25	10–35	$>$ 100	$<$ 15	60 s
Fine treatment side	Hydrogen conductivity at the A/B/C mixed-bed outlet	Fine Treatment System	$\geq$0.20; protection triggered at $>$ 0.25	10–35	$>$ 100	$<$ 15	60 s

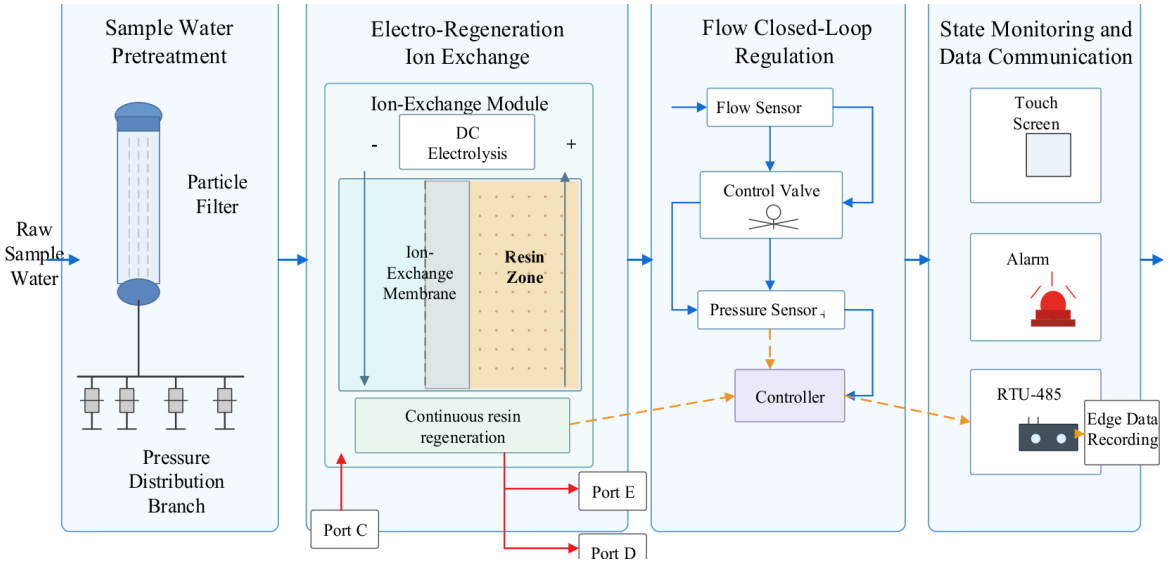

FIGURE 1. Overall Architecture of the Automated Ion Exchange System

migration of ions across the membrane. The controller increases the regeneration voltage or adjusts the variable frequency output when the specific conductivity of the sample water is increased or the NH4+ is increased, so as to keep sufficient migration driving on the two sides of the exchange membrane. In the literature, the device produces H+, and OH-, which are continuously regenerated by the exchange membrane, with a target cation removal rate of 99.9% or more [13].

In the closed loop control, the regeneration flow rate is the main control variable, and the waste water flow and pressure are the limiting variables. The regeneration flow rate setpoint Q_s is set based on the water quality load zones at each monitoring point: 80–100 mL/min for low-load monitoring points, 100–120 mL/min for medium-load monitoring points, and 120–150 mL/min during startup or periods of high ammonia disturbance; the wastewater channel is maintained at 50–150 mL/min to prevent the retention of exchange ions due to insufficient discharge. The flow deviation is defined as:

$$e_Q(t) = \frac{Q_s - Q_r(t)}{Q_s} \tag{2}$$

where $e_Q(t)$ is the relative deviation of the regeneration flow rate at time t; Q_s is the setpoint for the regeneration flow rate; and $Q_r(t)$ is the regeneration flow rate measured in real time by the flow sensor. The controller calculates $e_Q(t)$ every 5 s. When $|e_Q(t)| \leq 5\%$, the current valve position is maintained; when $|e_Q(t)| > 5\%$ and this condition persists for 30 s, the system enters the control state.

The control valve opening or micro-pump duty cycle is corrected using a clipped PID:

$$u(t) = K_p e_Q(t) + K_i \int_{t-\tau}^{t} e_Q(\xi) d\xi + K_d \frac{de_Q(t)}{dt} \tag{3}$$

where $u(t)$ is the correction value for the control valve opening or the pump output duty cycle; K_p, K_i, and K_d are the proportional, integral, and derivative coefficients, respectively; τ is the integral window length, set to 60–180 s; and ξ is the integral variable. To prevent false disturbances in hydrogen conductivity measurements caused by rapid

flow fluctuations, the controller sets a single-step correction limit for $u(t)$, ensuring that the valve position change does not exceed 5%, and establishes an 180-second stabilization observation window. The regeneration PIV values are associated with voltage, current, and active channel status to determine if the electric regeneration load is in line with the ion load of the sample water, thus avoiding long term under-regeneration or over-regeneration [14]. The device manual specifies a flow rate of 50 to 150 ml/min, a sample water pressure above 0.2 MPa, and a mean operating power of about 8 W. These can be used as a closed loop control boundary.

D. FAULT DIAGNOSIS AND PROTECTION LOGIC

Fault diagnosis uses an edge control logic that follows the sequence "threshold determination — state machine transition — event log locking — response prompt output," without relying on complex model training. The controller carries out parallel scanning of pressure, regeneration flow, waste water flow, voltage, current, PIV, touch screen mode, and communication state. Protection variables are sampled at 1-5 s intervals, and process variables are recorded at 60 s intervals. Water supply interruption, pressure loss, over-pressure, low flow, abnormal sewage discharge, abnormal power supply, and malfunction of maintenance mode are all independent states. All states are written into the Local Event Log and uploaded through RTU-485 [15] to the Chemical Monitoring Data Terminal.

Fault diagnosis employs a weighted status scoring system:

$$D(t) = \sum_{i=1}^{n} \alpha_i I[x_i(t) \notin (L_i, U_i)] + \sum_{j=1}^{m} \beta_j I[|\Delta x_j(t)| > \delta_j] \tag{4}$$

where $D(t)$ is the fault diagnosis score at time t; $x_i(t)$ is the i-th monitored variable; L_i and U_i are the lower and upper permissible limits of that variable, respectively; $I(\cdot)$ is an indicator function that takes the value 1 if the condition is met and 0 otherwise; $\Delta x_j(t)$ is the short-term variation of the j-th variable; δ_j is the variation threshold; α_i, β_j is the variable weight. Pressure, flow, and power-related variables are assigned higher weights, while communication and display-related variables are assigned lower weights. When $D(t)$ reaches the alarm threshold, the system latches the alarm; When the pressure is greater than 0.25 MPa, the system goes into overpressure stabilization protection; the regeneration is suspended and the low pressure warning is activated when the inlet water pressure is less than 0.20 MPa or the sample is interrupted for 10 seconds; if the flow is below the lower limit and is maintained for more than a predetermined time, the system shuts down the regeneration output to avoid drying the exchange membrane [16]. This logical configuration is supported by the device specification, which includes threshold values for self-diagnostic, water-supply, power-off, over-pressure, and flow-rate alarms.

E. ENERGY-SAVING POTENTIAL EVALUATION INDICATORS

The energy saving potential is assessed on the basis of a set of indicators that includes "the consumption of resources in the pre-measurement process — the power consumption during the automatic operation — the maintenance labor hours — the stability of the measurement." Resource consumption indicators include the amount of resin exchange, hydrochloric acid consumption, rinsing water volume, and waste liquid discharge; the operating indicators include the power consumption of the automation system, the deviation of the regeneration flow, the uptime of the instrument, and the alarm response time; the measurement indexes include the removal rate, the stabilization time of the hydrogen conductivity, the time for the stabilization of the hydrogen conductivity, and the change of the hydrogen conductivity. In this way, the implicit energy consumption of conventional cation exchange resin columns is included in the assessment, thus avoiding the narrow scope of energy savings resulting from a simple comparison of the energy consumption of automatic devices [17].

The cation removal rate is used to characterize the effectiveness of automated ion exchange in the pretreatment of hydrogen conductivity:

$$\eta_i = \left(1 - \frac{C_{out,i}}{C_{in,i}}\right) \times 100\% \tag{5}$$

where η_i is the removal rate of cation class i; $C_{in,i}$ is the concentration of cation class i before entering the ion exchange unit; and $C_{out,i}$ is the concentration of cation class i after treatment. NH4+ serves as the primary verification target, while Na+, Ca2+, and Mg2+ serve as secondary targets; the removal rate threshold is set at 99.9% for verification.

Hydrogen conductivity stability is expressed using the coefficient of variation:

$$CV_\kappa = \frac{\sigma_\kappa}{\bar{\kappa}} \times 100\% \tag{6}$$

where CV_κ is the coefficient of variation of hydrogen conductivity; σ_κ is the standard deviation of hydrogen conductivity within the stable operation window; and $\bar{\kappa}$ is the mean hydrogen conductivity within the same window. In order to filter short term sampling and single point interference, the window is set to 30 minutes [18].

The resource reduction rate is used to standardize indicators with different units of measurement, such as resin, hydrochloric acid, water, and labor hours:

$$R_m = \frac{X_{0,m} - X_{1,m}}{X_{0,m}} \times 100\% \tag{7}$$

In the equation, R_m represents the reduction rate for the mth category of resources or maintenance costs; $X_{0,m}$ represents the annual consumption under the traditional resin column process; and $X_{1,m}$ represents the annual consumption under the automated ion exchange system [19].

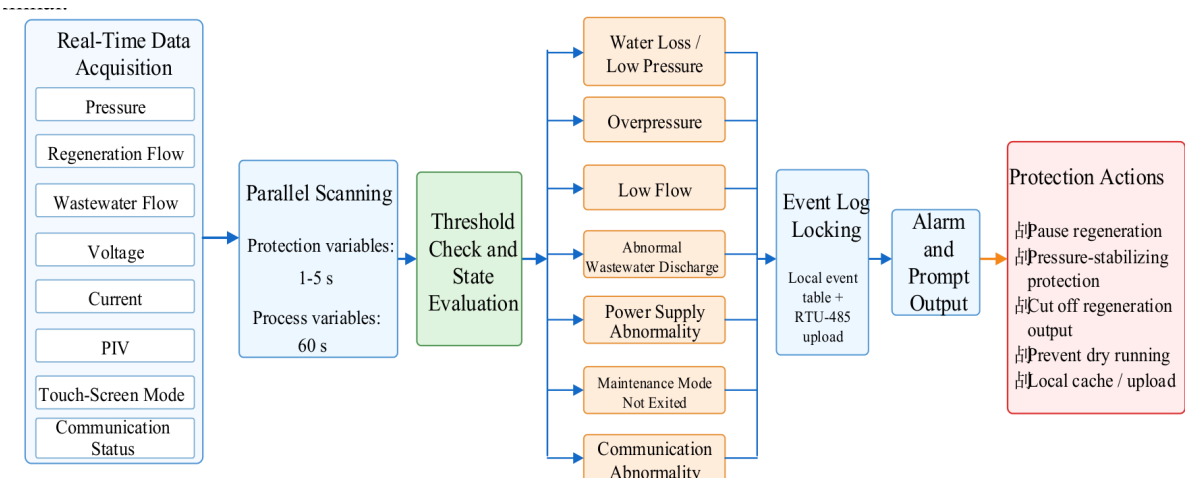

FIGURE 2. Fault Diagnosis and Safety Protection Logic Diagram

Traditional processes include manual regeneration, resin replacement, concentrated hydrochloric acid consumption, and backwashing processes; an automatic system that uses continuous electrical generation converts these items into annual comparable quantities. Specific indicators are shown in Table 2.

F. METHODOLOGY FOR CALCULATING ENERGY-SAVING BENEFITS

Energy efficiency is calculated on three levels: single measuring point, single unit, and whole plant. The calculation range of individual measuring points includes resin consumables, hydrochloric acid chemicals, washing water, waste fluid treatment, manual maintenance, and power consumption of the automation system; at unit level, data are aggregated on the basis of similar measuring points; at plant level, data are aggregated from 20 measuring points in units 1 and 3. Traditional process costs C_0 and automation system operating costs C_1 are expressed as follows:

$$C_0 = \sum_{m=1}^{k} p_m X_{0,m} + p_L H_0 + C_{w,0} \tag{8}$$

where C_0 is the annual operating cost of the traditional cation resin column process; C_1 is the annual operating cost of the automated ion exchange system; p_m is the unit price of resource category m; $X_{0,m}$ and $X_{1,m}$ are the annual consumption of resource category m before and after deployment, respectively; p_L is the unit price of labor hours; H_0 and H_1 are the annual maintenance labor hours before and after deployment, respectively; $C_{w,0}$ and $C_{w,1}$ are the waste liquid disposal costs before and after deployment, respectively; p_e represents the electricity price; E_{auto} represents the annual electricity consumption of the automation system. According to the data, traditional hydrogen conductivity meters require monthly maintenance across the entire plant, taking 2–3 workdays per month, or approximately 24–36 workdays per year, which can serve as the baseline for H_0.

The automation system's power consumption is calculated based on continuous operation:

$$E_{auto} = \sum_{r=1}^{N} P_r T \tag{9}$$

Where N represents the number of automated ion-exchange units; P_r represents the average operating power of the rth unit; and T_r represents the annual operating time of the rth unit. If the LZBP-08 unit is used, the average running power is 8W, and the annual running time is 8,760 hours. The annual net energy savings and energy savings per measuring point are calculated as follows:

$$B_{net} = C_0 - C_1 \tag{10}$$

$$B_s = \frac{B_{net}}{N_s} \tag{11}$$

In the formula, B_{net} represents the annualized net energy-saving benefit; B_s represents the annual energy-saving benefit per monitoring point; and N_s represents the number of hydrogen conductivity monitoring points included in the calculation. The payback period is calculated using the following formula:

$$T_p = \frac{I_0}{B_{net}} \tag{12}$$

In the equation, T_p represents the payback period; I_0 represents the one-time investment in the automated ion-exchange system equipment, installation, commissioning, and data integration. Existing research shows that the cost per unit of conventional resin is about 100,000 to 150,000 yuan per year, with the adoption of the intelligent system, the running costs can be reduced by 100,000 to 150,000 yuan. This margin is used to set the limits of the economic

TABLE 2. Evaluation indicator system for energy-saving potential

Indicator Level	Evaluation Indicator	Calculation or Data Collection Method	Unit	Purpose of Evaluation
Ion Exchange Performance	NH_4^+ Removal Efficiency	Calculation of Inlet and Outlet Ion Concentrations	%	Verification of Pretreatment Capacity
Ion Exchange Performance	Regeneration Flow Rate Deviation	Calculation of Set Flow Rate vs. Measured Flow Rate	%	Assessing Closed-Loop Control Stability
Measurement Stability	Hydrogen Conductance Fluctuation Coefficient	Calculation of Mean and Standard Deviation for a 30-Minute Window	%	Assessing the Degree of Continuous Measurement Stability
Measurement Stability	Stabilization time	Time Required to Enter the Permissible Fluctuation Range After Startup	min	Assessing the Burden of Flushing and Recovery
Resource Consumption	Resin consumption	Annual replacement or procurement volume statistics	kg/year or sets/year	Calculating Savings on Consumables
Resource Consumption	Hydrochloric acid consumption	Statistics on Regeneration Chemicals Ledger	kg/year or L/year	Calculate chemical savings
Resource Consumption	Flushing Water Volume	Integral of Flow Rate and Flushing Time	m^3/a	Calculate reduction in water consumption
Maintenance Costs	Manual maintenance hours	Calculation of Maintenance Personnel and Work Hours	h/a	Calculated Labor Savings
Operating Costs	Automation System Power Consumption	Power and Operating Time Calculation	kWh/a	Offset for Additional Electricity Consumption
Comprehensive Indicators	Comprehensive Energy-Saving Potential Index	Weighted Comprehensive Calculation	%	Aggregation of Multidimensional Energy-Saving Potential

sensitivity analysis and is not used as an outcome value directly [20]. Specific parameters are shown in Table 3.

III. RESULTS

A. SYSTEM CONTINUOUS OPERATIONAL STABILITY

Continuous operation validation was carried out with 20 measuring points for hydrogen conductivity, and the trial running time was set at 30 days. At the same time, the Edge Data Acquisition Module recorded the regeneration flow rate, the wastewater flow rate, the sample water pressure, the PIV, the voltage, the current, the warning event, and the data upload completion rate. Specific results are shown in Table 4.

In Table 4, the mean regeneration flow rate was 118.6 ml/min at 4.7 ml/min, both of which were within the specified range; the highest PSI was 0.252 MPa, triggering three short time pressure-stabilizing protective events, none of which led to a shutdown. There were 4 low flow alerts, 3 overpressures, and 1 communication buffer events, all of which were recorded by the controller and uploade.As illustrated in Figure 3, the flow rate of regeneration showed regulation oscillations from Day 1 to Day 3, and then stabilized at 115 to 123 ml/min; after a load disturbance, the PIV curve showed a slight rise, with the voltage curve rising in tandem, and the data upload completeness rate was consistently higher than 97%.

B. CATION REMOVAL AND HYDROGEN CONDUCTIVITY STABILITY

Cation removal efficiency was calculated based on the inlet and outlet concentrations of NH_4^+, While the time needed to achieve a steady state after start-up and the change coefficient in 30 minutes were used to assess the stability of hydrogen conductivity. Typical measuring points — including condensate pump outlet, deaerator inlet, economizer inlet, main steam, reheat steam, and fine processing outlet were chosen. This includes the high-ammonia feed side, the low-concentration steam side and the fine processing outlet side. The specific results are given in Table 5.

In Table 5, the NH_4^+ removal rates ranged from 99.90% to 99.94%, meeting the cation removal target of 99.9% or higher specified in the literature. The stabilization time for the automated system was 12–19 min, compared to 44–76 min for the traditional resin column; the coefficient of variation for hydrogen conductivity decreased from 6.1%–10.6% to 1.6%–2.7%.As shown in Figure 4, the NH_4^+ concentration at the feedwater-side monitoring point was relatively high, and the automatic system continued to show slight fluctuations for the first 10 minutes and then went into a steady phase of 15-20 minutes; the concentration at the steam side was lower and the curve was more rapid. The box and whisker plot shows a significant reduction in the hydrogen conductivity variation for the automatic system, with unusually high values occurring mainly at the inlet and outlet of the deaerator.

C. EFFECTS ON RESIN CONSUMPTION, ACID CONSUMPTION, AND FLUSHING WATER REDUCTION

Resource consumption was annualised on 20 measuring points. Pre-deployment data were collected from monthly resin regeneration or substitution records, hydrochloric acid usage records, estimated flushing water books, and waste liquid disposal records; post-deployment data included secondary filter maintenance, short flush, sewage discharge and reserve consumption. The automatic system produces H^+ by electrolysis of water, which is used for continuous resin regeneration, and does not involve the regeneration of hydrochloric acid. See Table 6 for a detailed comparison.

In Table 6, the consumption of hydrochloric acid was reduced from 480.0 l/year to 0, and the consumption of resin was reduced from 168.0 kg/year to 16.0 kg/year, which was 90.5%; the washing water consumption was reduced

TABLE 3. Calculation boundaries and parameter settings for energy-saving benefits

Parameter Category	Parameter Name	Symbol	Value or Setting Method	Data Source or Purpose
Number of Measurement Points	Number of Monitoring Points Included in the Assessment	Ns	20	On-site measurement points for Units 1 and 3
Automated Power Consumption	Average operating power per unit	Pr	8 W	Equipment Operating Parameters
Power consumption for automation	Annual operating time	Tr	8,760 h/a	Converted for continuous online operation
Resource Costs	Annual Resin Consumption	X0,resin, X1,resin	Pre- and Post-Deployment Ledger Statistics	Calculate Savings on Consumables
Chemical Costs	Annual hydrochloric acid consumption	X0,acid, X1,acid	Ledger Statistics Before and After Deployment	Calculate chemical savings
Water Consumption Costs	Flushing Water Volume	X0,water, X1,water	Flow Rate × Flushing Time	Calculate reduction in rinse water
Waste liquid cost	Waste liquid disposal cost	Cw,0, Cw,1	Waste liquid volume × disposal unit price	Calculate environmental disposal costs
Labor Costs	Annual Maintenance Hours	H0, H1	Number of employees × Maintenance duration	Calculate Labor Savings
Electricity Rate Parameters	Industrial electricity rate	pe	Based on the power plant's internal accounting rate	Offset against new electricity consumption
Investment Parameters	One-time investment	I0	Equipment + Installation + Commissioning + Communications	Calculate Payback Period

TABLE 4. Statistical results of key parameters during continuous operation

Parameter	Mean	Standard Deviation	Minimum	Maximum	Control Requirements
Sample water pressure / MPa	0.224	0.017	0.203	0.252	≥0.20; if it exceeds 0.25, protection is activated
Regeneration flow rate/(mL·min^{-1})	118.6	4.7	107.8	131.5	50–150
Wastewater flow rate/(mL·min^{-1})	104.3	5.8	91.2	119.6	50–150
PIV value	163.4	15.7	128.6	196.8	> 100
Regenerative voltage / V	16.7	1.9	12.4	21.3	5–24
Operating current/A	0.42	0.06	0.31	0.56	Stable Output
Data Completeness Rate (%)	98.7	0.6	97.2	99.5	≥ 95
Alarm events/occurrence	8	–	–	–	Event Latch Log

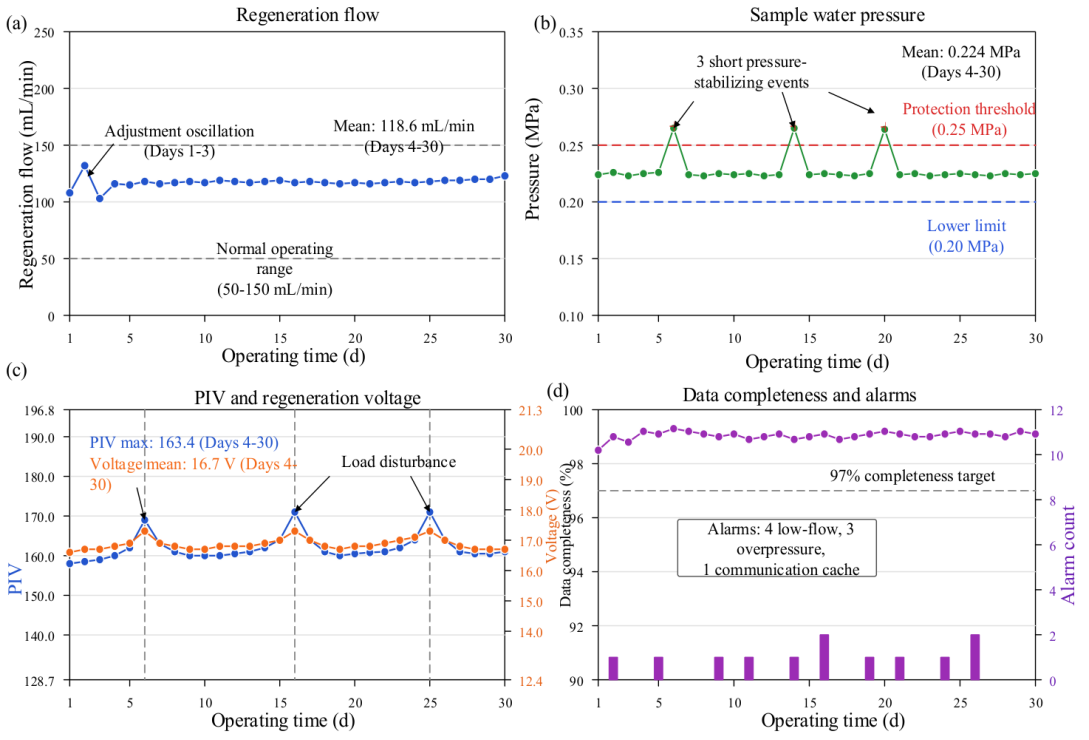

FIGURE 3. Changes in Continuous Operational Stability of the Automated Ion Exchange System

TABLE 5. Evaluation results for hydrogen conductance stability at different measurement points

Measurement Point	NH_4^+ Inlet Concentration/(μg·L^{-1})	NH_4^+ Removal Efficiency/%	Stabilization Time of Conventional Resin Column / min	Stabilization Time of Automated System (min)	CV of Conventional Measurement / %	CV of automated measurement/%
Condensate Pump Outlet	186	99.93	61	15	8.4	2.1
Deaerator inlet	318	99.91	76	19	10.6	2.7
Economizer inlet	274	99.92	69	17	9.8	2.5
Left side of main steam	42	99.9	48	13	6.7	1.8
Right side of main steam	39	99.91	46	12	6.4	1.7
Reheated steam, left side	35	99.9	44	12	6.1	1.6
Reheated steam, right side	37	99.9	45	13	6.3	1.7
Total fine processing outlet	126	99.94	58	14	7.9	1.9

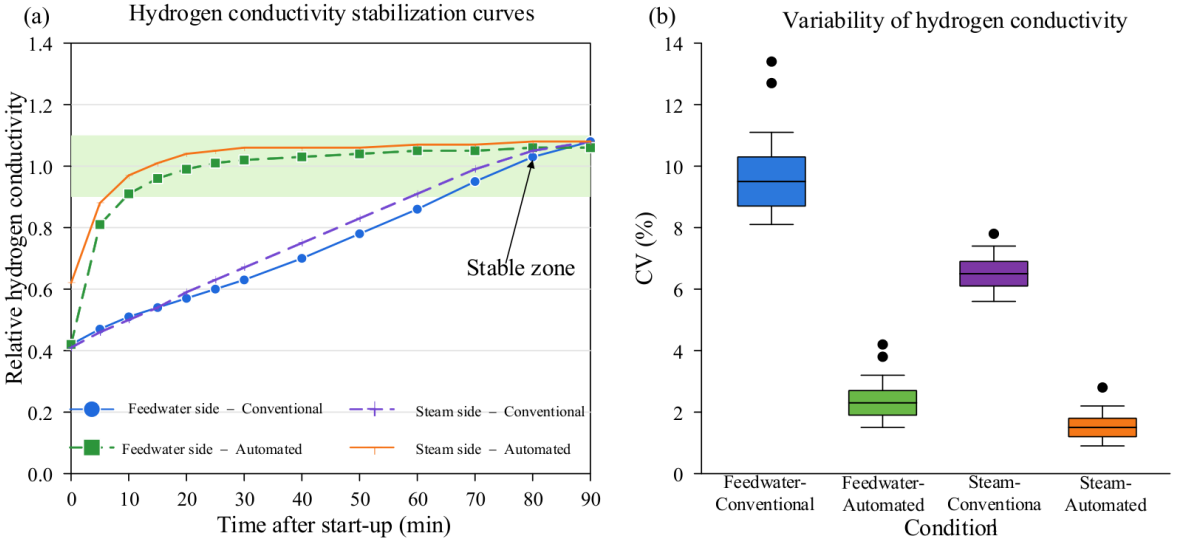

FIGURE 4. Comparison of Cation Removal Efficiency and Hydrogen Conductivity Stabilization Performance

TABLE 6. Comparison of resource consumption before and after deployment

Resource Item	Before Deployment	After Deployment	Reduction	Reduction Rate (%)	Statistical Basis
Cation resin consumption/(kg·a^{-1})	168	16	152	90.5	Annualized data from 20 monitoring sites
31% hydrochloric acid consumption/(L·a^{-1})	480	0	480	100	Regeneration Chemicals Ledger
Flushing Water Volume/(m^3·a^{-1})	42.6	9.4	33.2	77.9	Flow Rate × Flushing Time
Volume of regeneration waste liquid/(m^3·a^{-1})	3.2	0.64	2.56	80	Waste Liquid Collection Records
Secondary Filter Consumables/(sets·year^{-1})	0	40	Increase by 40	–	New maintenance items added after deployment
Number of short-term emissions/(times·a^{-1})	240	52	188	78.3	Maintenance Event Log

from 42.6 m ^{3}/year to 9.4 m ^{3}/a, the remainder being mainly due to the commissioning of the rinses and the short backwashing after the second filtration maintenance.The amount of the regeneration effluent was reduced from 3.20 m ^{3}/a to 0.64 m ^{3}/a. From top to bottom, as shown in Figure 5, the decrease in resource consumption is as follows: hydrochloric acid, resin, effluent, and rinse water. While the second type of filter is a new addition, it represents a small part of the decrease in acid consumption, resin and wash water, and does not change the general trend of resource consumption.

D. REDUCTION IN MANUAL MAINTENANCE HOURS

Manual maintenance was classified into six categories: "Regeneration preparation, Resin Disassembly and Assembly, Acid Cleaning and Regeneration, Column Loading and Washing, Instrumentation Validation, and Abnormal Treatment." Traditionally, Maintenance was carried out on a monthly basis, which was equivalent to 2-3 workdays for the whole factory, and thus had 288 hours of maintenance work per year. Following the deployment of the automation system, on-site operations were reduced to a touch screen check, a second filter check, an alarm event check, and a quarterly calibration, resulting in 62 hours of maintenance work. Based on the data, the conventional approach requires a minimum of 24 – 36 working days per year for the maintenance of the HCI, which is in line with this calculation. As illustrated in Fig. 6, the number of working hours for resin regeneration and column washing was reduced from 192 hours per year to 0; routine inspections were reduced

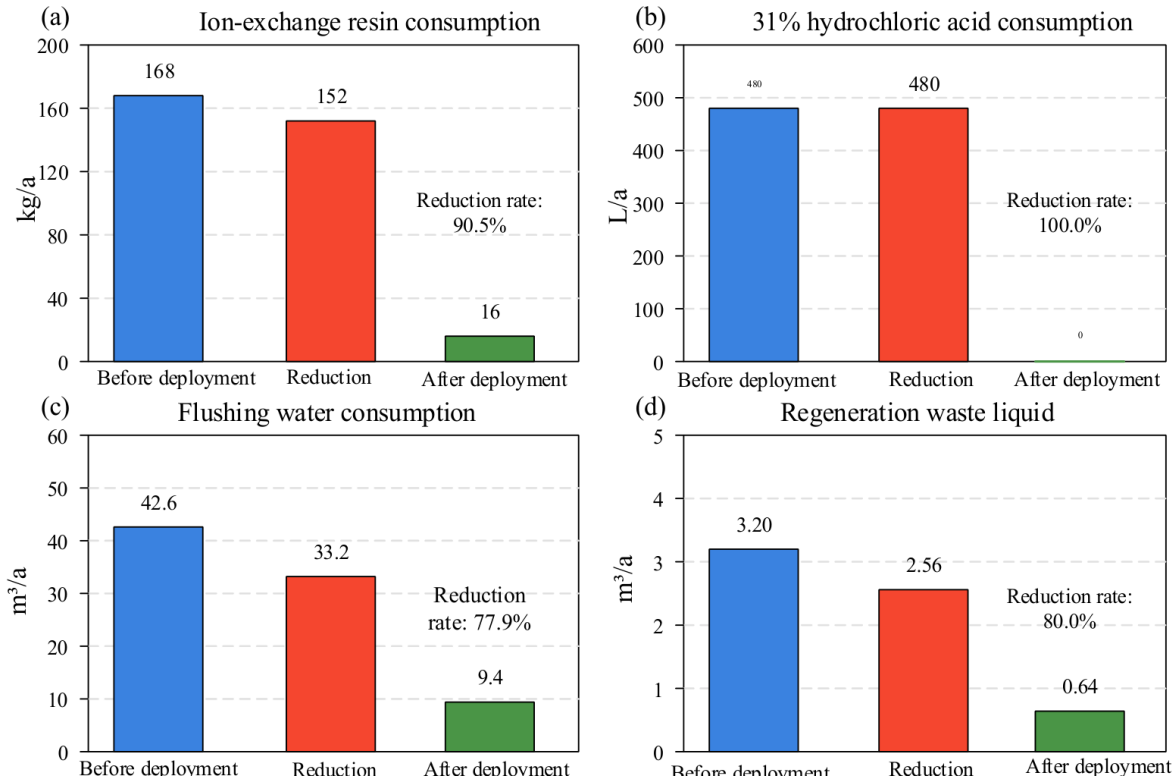

FIGURE 5. Reduction in Resin, Hydrochloric Acid, Rinse Water, and Waste Liquid

from 48 hours per year to 36 hours per year, and abnormal treatment was reduced from 48 hours per year to 26 hours per year. The event column in the diagram shows that the filter maintenance and alarm validation tasks are maintained after deployment; the manual maintenance workload has not been lowered to zero.

E. RESULTS OF THE COMPREHENSIVE ENERGY-SAVING POTENTIAL ASSESSMENT

The total energy saving potential was calculated on the basis of an annualised cost difference, including resin, hydrochloric acid, rinse water, waste fluid treatment, manual maintenance, second filter consumption, and power consumption of the automation system, which was calculated on the basis of 20 units running continuously, with an average operating power of 8 W per unit, and 8 760 hours per year running, generating an annual power consumption of 1,401.6 kWh. This power is in agreement with the mean power of the equipment manual. The overall energy saving potential evaluation results are presented in table 7.

In Table 7, the annual operating and maintenance cost of 20 monitoring stations was 16.68 RMB before deployment and 2.36 RMB after deployment, which is a net decrease of 14.32 RMB per year and 85.9% decrease in total. Based on an estimated one time investment of 360,000 CNY, the static payback period is 2.51 years. The data shows that the maintenance costs of conventional hydrogen-conductive resin units are about 100,000 to 150,000 CNY, and the automatic system saves about 100,000 to 150,000 CNY annually; this is within the reference range. As illustrated in Fig. 7, the largest contribution was from resin consumables, which accounted for 79.6 per cent of the net energy efficiency, and 14.2 per cent of work-related maintenance; and 9.6 per cent of hydrochloric acid, effluent, and wash-water; and the secondary filter and automatic power consumption, which were treated as offsets, accounted for 3.4 per cent. The waterfall diagram in the drawing shows that the additional power consumed by the automation system has little effect on the annual net profit, while the energy saving potential is mainly due to the reduction in the resource consumption of the conventional resin column.

IV. DISCUSSION

Continuous electro-regeneration mechanism is the essence of a new working principle of conventional hydrogen conductivity pretreatment system. The performance of traditional cation exchange resin column in a batch operation of exhaustion, removal, acid regeneration, reloading and rinsing depends significantly on the quality of regeneration, packing density of resin, and completeness of rinsing. The proposed system allows, on the contrary, a continuous regeneration, obtained by producing H+ by electrolysing water in the presence of a direct current field and by regenerating the ion-exchange capacity by selective transport of the membranes. This transformation enables stable operation even at high NH_4^+ loading and makes it possible to op-

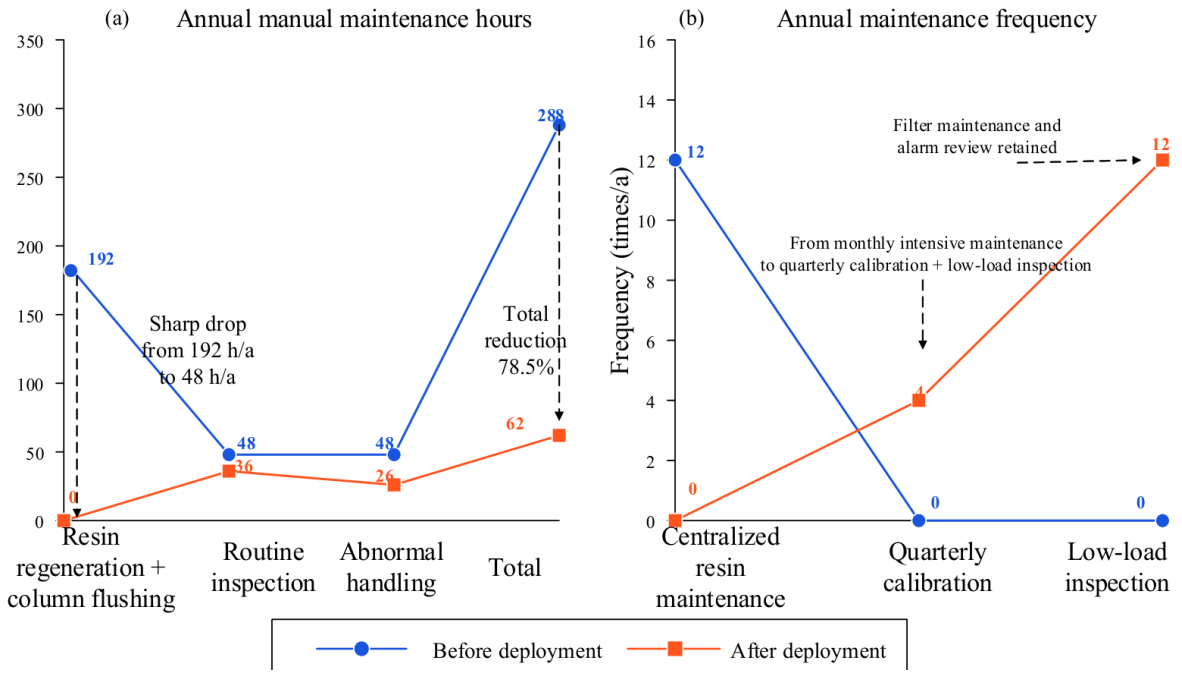

FIGURE 6. Effect of Reduced Manual Maintenance Hours and Maintenance Frequency

TABLE 7. Results of the comprehensive energy-saving potential assessment for the automated ion exchange system

Cost Item	Cost Before Deployment/(10,000 yuan·a^{-1})	Cost After Deployment/(10,000 yuan·a^{-1})	Net Reduction/(10,000 yuan·a^{-1})	Reduction Rate (%)
Resin Consumables	12.6	1.2	11.4	90.5
Hydrochloric acid reagent	0.96	0	0.96	100
Rinse water	0.05	0.01	0.04	80
Waste liquid disposal	0.48	0.1	0.38	79.2
Manual maintenance	2.59	0.56	2.03	78.4
Secondary filter media	0	0.4	-0.4	–
Power Consumption During Automated Operation	0	0.09	-0.09	–
Total	16.68	2.36	14.32	85.9

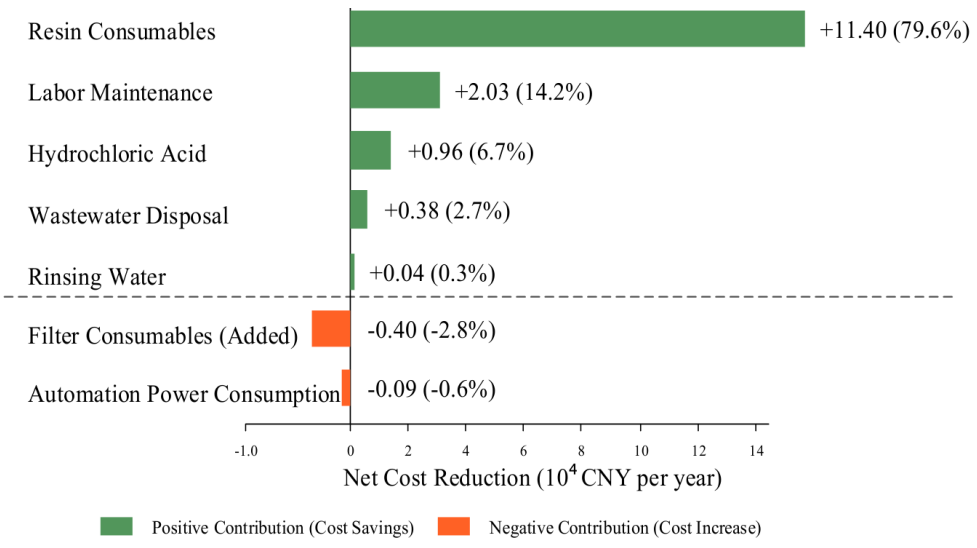

FIGURE 7. Analysis of Contributions to Comprehensive Energy-Saving Benefits

erate the process from experience-dependent operation to a parameter-controlled electrochemical system with capability of real-time monitoring.

In closed flow control measurements, the stability is sig-

nificantly important. The conductivity of hydrogen depends on the flow rate, the time of contact with the resin and the discharge behavior during regeneration. If the flow is too low, then there is a delay in the response, whereas if the flow is too great, then the ion exchange efficiency reduces. Regeneration flow is controlled by the system with the feedback obtained from the flow sensors, control valves and PIV signals to counteract pressure and ionic load changes. This approach minimizes the conductivity drift on start up and load disturbances over constant voltage or manual control. Edge data acquisition allows for simultaneous recording of pressure, flow, voltage, current and alarms, which allows for traceable process monitoring and operational profiling. The potential for energy saving is primarily put on optimizing the chain of use of resources, but not on reducing electrical energy consumption directly. While an extra cost is a power consumption due to the continuous operation, it is small compared with the operational cost of a year. The advantages are considerable reductions in the use of resin replacement, elimination of the need for acid regeneration, use of less rinsing water, less waste liquid discharge and less manual maintenance. Scale effects enhance these reductions in multi-point monitoring systems. Thus, evaluation needs to incorporate consumables, chemicals, water consumption, labor and downtime to ensure a true system level efficiency. (4) Limitations are the relatively short 30-day validation period (not a long term aging of the membrane, fouling by resin or degradation of the performance under frequent start-stop or high load situation). Furthermore, high hardness, residual chlorine, heavy metals or TOC levels may also lead to a higher fouling risk with a need for higher pretreatment measures if exposure is sustained. Payback estimates are based on annualized assumptions and large differences in monitoring scale, material cost and frequency of maintenance will influence the cost of the system. Future study should include the validation in full-cycle operation and abnormal water-quality conditions for more robustness of the proposed model.

V. CONCLUSION

The study shows that the automated electro-regenerated ion exchange system can greatly improve the stability of hydrogen conductivity measurement, and reduce the consumption of chemicals and workload in water – steam systems of thermal power plants. The system can operate continuously with high ion removal efficiency, which eliminates the need for traditional acid-regenerated resin system. The results show that measurement stability is highly sensitive towards pretreatment continuity and the proposed system is capable of solving the problems of conventional resin columns. The results agree with recent research on electrically driven ion transport systems and expand the use of the same systems to the field level water–steam monitoring. Future research should be directed towards long-term stability in operation, ageing behavior of membrane and adaptive control optimization for different water chemistries.

REFERENCES

[1] Y. Nakatsuchi, A. Hamasaki, H. Kido, et al., "Novel identification method of seawater contamination in the steam-water circuit, including carbon dioxide, in power plants based on pH, specific conductivity, and cation conductivity," *J. Chem. Eng. Jpn.*, vol. 56, no. 1, Art. no. 2238770, 2023, doi: 10.1080/00219592.2023.2238770.

[2] S. Vidojkovic, M. Mijajlovic, R. E. F. Lindeboom, et al., "Thermal stability of film-forming amine-based corrosion inhibitors in high-temperature power plant water solutions," *Energy Sci. Eng.*, vol. 12, no. 1, pp. 304–328, 2024, doi: 10.1002/ese3.1625.

[3] N. Ida, J. Tani, and H. Kawamura, "Applicability of hydrazine alternatives to water treatment in power plants: Effects of hydrazine alternatives and decomposition products on water properties and corrosion of carbon steel," *Corrosion*, vol. 80, no. 11, pp. 1069–1080, 2024, doi: 10.5006/4621.

[4] C. Cassaro, G. Virruso, A. Culcasi, et al., "Electrodialysis with bipolar membranes for the sustainable production of chemicals from seawater brines at pilot plant scale," *ACS Sustain. Chem. Eng.*, vol. 11, no. 7, pp. 2989–3000, 2023, doi: 10.1021/acssuschemeng.2c06636.

[5] M. Herrero-Gonzalez, J. López, G. Virruso, et al., "Analysis of operational parameters in acid and base production using an electrodialysis with bipolar membranes pilot plant," *Membranes*, vol. 13, no. 2, Art. no. 200, 2023, doi: 10.3390/membranes13020200.

[6] G. Virruso, C. Cassaro, A. Tamburini, et al., "Performance evaluation of an electrodialysis pilot plant with bipolar membranes operated in feed & bleed mode," *Chem. Eng. Trans.*, vol. 105, pp. 73–78, 2023, doi: 10.3303/CET23105013.

[7] Ö. Tekinalp, P. Zimmermann, S. Holdcroft, et al., "Cation-exchange membranes and process optimizations in electrodialysis for selective metal separation: A review," *Membranes*, vol. 13, no. 6, Art. no. 566, 2023, doi: 10.3390/membranes13060566.

[8] S. Kikuchi, S. Hirao, S. Kayakiri, et al., "Study on efficient operating conditions for bipolar membrane electrodialysis using different ion species and anion-exchange membranes," *Membranes*, vol. 14, no. 12, Art. no. 262, 2024, doi: 10.3390/membranes14120262.

[9] G. Hopsort, Q. Cacciuttolo, and D. Pasquier, "Electrodialysis as a key operating unit in chemical processes: From lab to pilot scale of latest breakthroughs," *Chem. Eng. J.*, vol. 494, Art. no. 153111, 2024, doi: 10.1016/j.cej.2024.153111.

[10] S. K. Patel, B. Lee, P. Westerhoff, et al., "The potential of electrodialysis as a cost-effective alternative to reverse osmosis for brackish water desalination," *Water Res.*, vol. 250, Art. no. 121009, 2024, doi: 10.1016/j.watres.2023.121009.

[11] J. T. Y. Bessette, S. R. Pratt, and V. A. G. Winter, "Direct-drive photovoltaic electrodialysis via flow-commanded current control," *Nat. Water*, vol. 2, no. 10, pp. 1019–1027, 2024, doi: 10.1038/s44221-024-00314-6.

[12] S. Sanjay and K. Jayamoorthy, "Sustainable desalination through electrodeionization: Innovations and focus on efficient carbonate ion removal—a comprehensive review," *Environ. Technol. Rev.*, vol. 13, no. 1, pp. 699–721, 2024, doi: 10.1080/21622515.2024.2417852.

[13] A. A. Oladipo and M. Ahmad, "Energy-efficient ion recovery from water using electro-driven membranes: A comprehensive critical review," *Water*, vol. 17, no. 16, Art. no. 2456, 2025, doi: 10.3390/w17162456.

[14] M. Miller, A. Kisiel, D. Cembrowska-Lech, et al., "IoT in water quality monitoring—Are we really there yet?" *Sensors*, vol. 23, no. 2, Art. no. 960, 2023, doi: 10.3390/s23020960.

[15] Y. Singh and T. Walingo, "Smart water quality monitoring with IoT wireless sensor networks," *Sensors*, vol. 24, no. 9, Art. no. 2871, 2024, doi: 10.3390/s24092871.

[16] M. Kumar, K. Khamis, R. Stevens, et al., "In-situ optical water quality monitoring sensors—applications, challenges, and future opportunities," *Front. Water*, vol. 6, Art. no. 1380133, 2024, doi: 10.3389/frwa.2024.1380133.

[17] K. Lal, S. Menon, F. Noble, et al., "Low-cost IoT-based system for lake water quality monitoring," *PLoS ONE*, vol. 19, no. 3, Art. no. e0299089, 2024, doi: 10.1371/journal.pone.0299089.

[18] M. A. Murti, A. R. A. Saputra, I. Alinursafa, et al., "Smart system for water quality monitoring utilizing long-range Internet of Things," *Appl. Water Sci.*, vol. 14, no. 4, Art. no. 69, 2024, doi: 10.1007/s13201-024-02128-z.

[19] P. Chandramenon, A. Gascoyne, L. Naughton, et al., "Making aquaponics more sustainable using worms and water replenishment combined with a sensing- and IoT-based monitoring system," *Appl. Sci.*, vol. 14, no. 18, Art. no. 8516, 2024, doi: 10.3390/app14188516.

[20] S. Khalid, J. Song, I. Raouf, et al., "Advances in fault detection and diagnosis for thermal power plants: A review of intelligent techniques," *Mathematics*, vol. 11, no. 8, Art. no. 1767, 2023, doi: 10.3390/math11081767.